International Journal of Aeronautical and Space Sciences (2021) 22:1170–1182
https://doi.org/10.1007/s42405-020-00347-7

IJASS International Journal of Aeronautical and Space Sciences

ORIGINAL PAPER


# A New Guidance Algorithm Against High-Speed Maneuvering Target

**Kyoung-Rok Song[1] · Tae-Hun Kim[2] · Chang-Hun Lee[1] · Min-Jea Tahk[1]**

Received: 3 March 2020 / Revised: 23 September 2020 / Accepted: 18 December 2020 / Published online: 22 January 2021


**Abstract**
This paper aims to propose a new guidance algorithm for intercepting a high-speed maneuvering target, such as a tactical ballistic missile that flies in a quasi-ballistic trajectory. The motivation of this study lies in the fact that the classical proportional navigation guidance (PNG) undergoes the performance degradation under the above engagement scenario due to its intrinsic property. To deal with the issue, an accurate collision course that reflects the motion characteristics of the ballistic target and missile is first analyzed. The desired look angle that leads to achieving the accurate collision course is then determined with the help of a novel time-to-go calculation method. Finally, the proposed guidance law providing the desired look angle is obtained by leveraging the concept of the biased PNG. Since the proposed method is designed to achieve an accurate collision course, it does not lead to unnecessary maneuvering near the target under the engagement scenario. This property is desirable for reserving the operational margin of maneuverability for reacting to unexpected situations during the engagement. It could improve the capturability of the target. Finally, the performance of the proposed method is verified through numerical simulations in a way to compare with the existing methods such as PNG and the augmented PNG (APNG).

**Keywords** Homing guidance · A high-speed maneuvering target · Ballistic threat · Biased PNG

## 1 Introduction

The classical proportional navigation guidance (PNG) [1] has been widely adopted as the terminal homing guidance for various guided weapon systems because of its favorable characteristics. First, the guidance command of PNG is given in a simple form multiplied by the line-of-sight (LOS) rate and the closing velocity between a missile and a target. Additionally, it has been proven that PNG can guarantee the optimality from the control energy minimization standpoint through the optimal control theory [2–6].

The underlying principle of PNG is to nullify the LOS rate in a finite time to accomplish a specific collision course, which is derived under the assumption that a missile and a target are moving at constant speeds [1]. Because of this inherent property of PNG, severe performance degradation would be expected under a specific engagement scenario where the underlying assumption of PNG does not hold. One example would be an engagement scenario for a tactical ballistic missile flying in a quasi-ballistic trajectory. In this scenario, a tactical ballistic target generally descends downward with a high speed of a few km/s, and it undergoes a nonlinear deceleration around 10–30 g caused by aerodynamic drag during its terminal homing phase. Additionally, a ballistic target could be performing lateral maneuvering up to 20 g intended to avoid an attack of an interceptor missile [7]. According to references [8, 9], under this extreme engagement case, PNG leads to large unnecessary maneuvering in the terminal homing phase. This large maneuvering may result in command saturations near the target so that severe miss distance may occur [10]. Thus, it can be predicted that the capture region of the ballistic target under PNG may be considerably reduced.

✉ Chang-Hun Lee
lckdgns@kaist.ac.kr

Kyoung-Rok Song
oracle61@kaist.ac.kr

Tae-Hun Kim
tehunida@gmail.com

Min-Jea Tahk
mjtahk@kaist.ac.kr

[1] Department of Aerospace Engineering, Korea Advanced Institute of Science and Technology(KAIST), 291 Daehak-ro, Yuseong-gu, Daejeon 34141, Korea

[2] Agency for Defense Development(ADD), Yuseong, P. O. Box 35, Daejeon 34186, Korea

Over the past several decades, various guidance laws have been proposed in consideration of target and missile motions to overcome the above issue. In the augmented proportional navigation guidance (APNG), which is one of the variations of PNG, the target lateral acceleration is added to the PNG command for reducing the required terminal acceleration. In reference [11, 12], a homing guidance law was proposed based on the optimal control, to compensate for speed variation due to a constant longitudinal acceleration of a missile. The authors in [13, 14] proposed a new homing guidance law that compensates for the speed variation of a target caused by its constant longitudinal acceleration in nonlinear engagement kinematics. In the previous study [15], a new homing guidance law was developed, which considered a nonlinear longitudinal acceleration of a missile caused by aerodynamic drag and thrust. A homing guidance law for an accelerating missile by a thrust operated in the exo-atmospheric region was suggested using the nonlinear control theory and the optimal control theory [16, 17]. The authors in [18] proposed an optimal guidance law that compensates for the speed variation of a missile by estimating a velocity profile in a real-time manner. In reference [22], a guidance algorithm that switches between PNG and APNG, depending on target maneuvers, was proposed. In reference [23], a novel head-pursuit guidance was developed for intercepting a high-speed target. This guidance law could significantly reduce the closing velocity, and this property helps relax the control energy requirement. For improving the kill probability against a high-speed target such as a ballistic missile, a simultaneous salvo attack algorithm based on retro-PN was studied in reference [24].

It is worth noting that although the above methods could provide better performance than the classical PNG by considering additional missile or target motions, each specific engagement scenario was assumed to design each guidance law. It implies that the above methods may not guarantee excellent performance in the engagement for the tactical ballistic missile that flies in a quasi-ballistic trajectory. This is because they were not inherently designed to focus on this specific engagement scenario mentioned above.

Based on this observation, this paper aims to propose a new homing guidance law that can drive the interceptor missile toward a more accurate collision course by fully utilizing the motion characteristics and the flight parameters of the quasi-ballistic target and the interceptor missile. To this end, the closed-form trajectory solutions of a conventional biased PNG (BPNG) law are first determined. From the results obtained, it turns out that the bias term of BPNG corresponds to the collision triangle. Based on these relations, the desired look angle providing an accurate collision course for a ballistic target is then derived using the linearized engagement kinematics under reasonable assumptions. Also, since the time-to-go information is required to determine the desired look angle, an accurate time-to-go calculation method is newly proposed in this paper. Finally, the state-feedback form of the guidance law achieving the desired look angle in a finite time is developed by utilizing the concept of the biased PNG.

Since the proposed guidance law places the missile on the accurate collision triangle, the acceleration demand in the terminal homing phase can be considerably reduced. This property of the proposed method could be desirable in terms of reserving some operational margin of maneuverability for coping with unexpected situations [19]. This characteristic is also desirable to avoid command saturations near a target [10]. Therefore, the proposed method could be advantageous in terms of providing a possibility to improve the capturability of the ballistic target, compared to PNG. To verify this fact, numerical simulations are performed. The results obtained show that the proposed method is superior to PNG and APNG.

This paper is organized as follows. In Sect. 2, the closed-form solutions and physical constraints for the biased PNG law are derived. In Sect. 3, the guidance problem to be solved in this study is introduced, and the proposed guidance algorithm with the time-to-go calculation method is discussed. In Sect. 4, numerical simulation results are presented. Finally, the concluding remark of this study is offered in Sect. 5.

## 2 Analysis of Biased PNG for Constant Maneuvering Targets

Before proposing a new guidance law against a high-speed maneuvering target, we first derive a closed-form trajectory solution for a conventional BPNG law against a constant maneuvering target. Based on the closed-form solution, we then find a significant physical constraint to achieve zero miss distance and zero terminal acceleration.

### 2.1 Linearized Engagement with Biased PNG

Let us consider the linearized kinematics depicted in Fig. 1 and the BPNG command given by Eq. (1).

$$a_m = N' v_c (\dot{\sigma} - \dot{\sigma}^*), \tag{1}$$

where $N'$, $v_c$, and $\dot{\sigma}$ are the effective navigation ratio, the closing velocity, and the line-of-sight (LOS) rate, respectively. The notation, $\dot{\sigma}^*$, denotes the desired LOS rate to be determined for satisfying the terminal constraints. In Fig. 1, other variables are self-explanatory.

As shown in Fig. 1, by assuming a near head-on engagement with constant speeds (i.e., $\dot{v}_m = 0$ and $\dot{v}_t = 0$) and

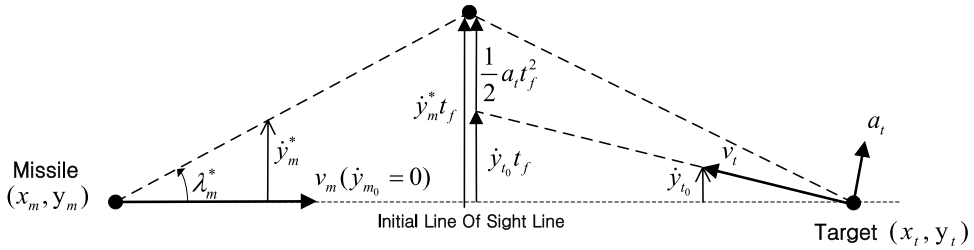


**Fig. 1** Linearized engagement geometry for BPNG

constant lateral acceleration of the target (i.e., $\dot{a}_t = 0$), the linearized engagement kinematics with respect to the initial LOS can be obtained as follows:

$$\begin{aligned}\ddot{y} &= \ddot{y}_t - \ddot{y}_m = a_t - a_m \\ &= a_t - N' v_c(\dot{\sigma} - \dot{\sigma}^*) = -N' v_c \dot{\sigma} + (a_t + N' v_c \dot{\sigma}^*).\end{aligned} \tag{2}$$

Here, the variables $y\dot{y}$, and $\ddot{y}$ represent the relative lateral position, velocity, and acceleration with respect to the initial LOS, and the initial conditions are given as

$$y_0 = 0, \quad \dot{y}_0 = \dot{y}_{t_0}. \tag{3}$$

And then, integrating Eq. (2) using the above initial conditions and the geometric relation $\sigma = y/v_c t_{go}$ gives

$$\dot{y} + \frac{N'}{t_{go}} y = Kt + \dot{y}_0, \tag{4}$$

where $K = a_t + N' v_c \dot{\sigma}^*$, and this is assumed to be constant for analysis purposes. Note that the above equation is the first-order ordinary differential equation (ODE).

## 2.2 Closed-form Trajectory Solutions to Biased PNG

By applying a general solution presented in [3] to the first-order ODE, as shown in Eq. (4), we can obtain the closed-form solution of the relative lateral position as follows:

$$y(t) = \frac{K t_f t}{N'-1}\left(\frac{t_f - t}{t_f}\right) - \frac{K t_f^2}{(N'-1)(N'-2)}\left[\left(\frac{t_f - t}{t_f}\right)^2 - \left(\frac{t_f - t}{t_f}\right)^{N'}\right] + \frac{\dot{y}_0 t_f}{N'-1}\left[\left(\frac{t_f - t}{t_f}\right) - \left(\frac{t_f - t}{t_f}\right)^{N'}\right]. \tag{5}$$

By differentiating Eq. (5) twice, we have

$$\ddot{y}(t) = -\frac{2K}{N'-1} - \frac{K}{(N'-1)(N'-2)}\left[2 - N'(N'-1)\left(\frac{t_f - t}{t_f}\right)^{N'-2}\right] - \frac{N'\dot{y}_0}{t_f}\left(\frac{t_f - t}{t_f}\right)^{N'-2}. \tag{6}$$

From the closed-form solution of the relative lateral position, as shown in Eq. (5), it can be observed that if there is no limitation on the missile acceleration, then the relative lateral position for $N' > 2$ always converges to zero (i.e., $y(t_f) = 0$) regardless of $a_t$ and $\dot{\sigma}^*$. Additionally, from Eq. (6), we can observe that the relative lateral acceleration converges to a specific value depending on $a_t$ and $\dot{\sigma}^*$. In other words, the zero terminal acceleration may not always be achieved for given $a_t$ and $\dot{\sigma}^*$. Therefore, it implies that an appropriate desired LOS rate should be determined to achieve the zero terminal acceleration.

From Eq. (6), we can obtain the relative lateral acceleration at the terminal time as

$$\ddot{y}(t_f) = a_t - a_m(t_f) = -\frac{2K}{N'-1} - \frac{2K}{(N'-1)(N'-2)} = -\frac{2K}{N'-2}. \tag{7}$$

By rearranging Eq. (7), the condition satisfying the zero terminal acceleration can be determined as

$$a_m(t_f) = 0 = a_t + \frac{2K}{N'-2} = \left(\frac{N'}{N'-2}\right) a_t + 2\left(\frac{N'}{N'-2}\right) v_c \dot{\sigma}^*. \tag{8}$$

By substituting the desired LOS rate definition, $\dot{\sigma}^* = (\dot{y}_{t_0} - \dot{y}_m^*) t_f / v_c t_f^2$ which is expressed by the desired lateral velocity of the missile $\dot{y}_m^*$ and the initial conditions, into Eq. (8), the above condition can be rewritten as

$$0 = a_t + 2 v_c \dot{\sigma}^* = a_t + 2 v_c \left[\frac{(\dot{y}_{t_0} - \dot{y}_m^*) t_f}{v_c t_f^2}\right] \quad \Rightarrow \quad \dot{y}_m^* t_f = \dot{y}_{t_0} t_f + \frac{1}{2} a_t t_f^2. \tag{9}$$

It is noted that the above equation represents an essential condition for determining a unique desired LOS rate providing the zero terminal acceleration. To be more specific, once $\dot{y}_m^*$ is determined from Eq. (9), $\dot{\sigma}^*$ ensuring the zero terminal acceleration can be obtained by the LOS rate definition (i.e., $\dot{\sigma}^* = (\dot{y}_{t_0} - \dot{y}_m^*) t_f / v_c t_f^2$). Finally, in a way to apply the

obtained $\dot{\sigma}^*$ to the BPNG command, as shown in Eq. (1), we can develop a guidance law providing the zero terminal acceleration against a maneuvering target. For instance, we can obtain $\dot{y}_m^* = \dot{y}_{t_0}$ for a non-maneuvering target (i.e., $a_t = 0$) from Eq. (9). In that case, based on the LOS rate definition, we can obtain the desired LOS rate providing the zero terminal acceleration as $\dot{\sigma}^* = 0$. Therefore, from Eq. (1) with $\dot{\sigma}^* = 0$, we can readily observe that the BPNG command for a non-maneuvering target can be converted into the conventional PNG law as $a_m = N' v_c \dot{\sigma}$. For a constant maneuvering target (i.e.,$a_t \neq 0$ and $\dot{a}_t = 0$), the desired lateral velocity and the desired LOS rate are determined as $\dot{y}_m^* = \dot{y}_{t_0} + 0.5 a_t t_f$ and $\sigma^* = -a_t / 2v_c$, from Eq. (9) and the LOS rate definition. Finally, the BPNG command with these solutions become $a_m = N' v_c \left( \dot{\sigma} + \frac{a_t}{2v_c} \right) = N' v_c \dot{\sigma} + \frac{N'}{2} a_t$, which is identical to APNG law.

The above result provides significant physical meaning and insight into the engagement condition for maneuvering targets. From Eq. (9) and Fig. 1, it can be observed that the desired lateral velocity $\dot{y}_m^*$ and the corresponding desired LOS rate $\dot{\sigma}^*$ should be determined to make the zero-effort-miss (ZEM) becomes zero. In other words, the physical meaning of $\dot{y}_m^*$ (or $\lambda_m^* \approx \dot{y}_m^* / v_m$) is the desired look angle corresponding to a collision course that makes a missile intercept a target without further corrective maneuvers. Therefore, based on this fact, we can design a BPNG-type guidance law minimizing the miss distance and the terminal acceleration demand. To be more specific, when an accurate collision triangle is predicted by utilizing a precise time-to-go calculation method and considering the motion characteristics of the missile and the target, the desired look angle providing the predicted collision course can then be determined. Finally, in a way to apply the desired LOS rate corresponding to the desired look angle into Eq. (1), a guidance law can be determined. In the next section, the proposed guidance law will be derived based on this design procedure.

## 3 Proposed Guidance Algorithm

In this section, the engagement kinematics used in this study is derived under some reasonable assumptions. By the engagement kinematics, the proposed guidance algorithm is then developed. First, a way to determine the desired look angle, achieving an accurate collision course that reflects the motion characteristics of the missile and target, is described. A new time-to-go calculation method for this engagement scenario is also explained. Finally, the proposed guidance law will be developed in the form of BPNG, based on the above information.

### 3.1 Engagement Kinematics

As shown in Fig. 2, we consider an engagement scenario for a surface-to-air missile against a high-speed maneuvering target, such as a tactical ballistic missile flying in a quasi-ballistic trajectory. Before developing the proposed guidance algorithm, the following assumptions are made for the engagement kinematics:

**Assumption 1** The missile and the target are treated as point-mass models.

**Assumption 2** The gravity acting on the missile and the target is omitted in the relative engagement kinematics. Additionally, the target parameters, such as the ballistic coefficient and the gravitational acceleration, are treated as constant values during the engagement.

**Assumption 3** The lateral acceleration of the target is treated as a constant value during the engagement.

**Assumption 4** The longitudinal acceleration of the missile is treated as a constant value during the engagement.

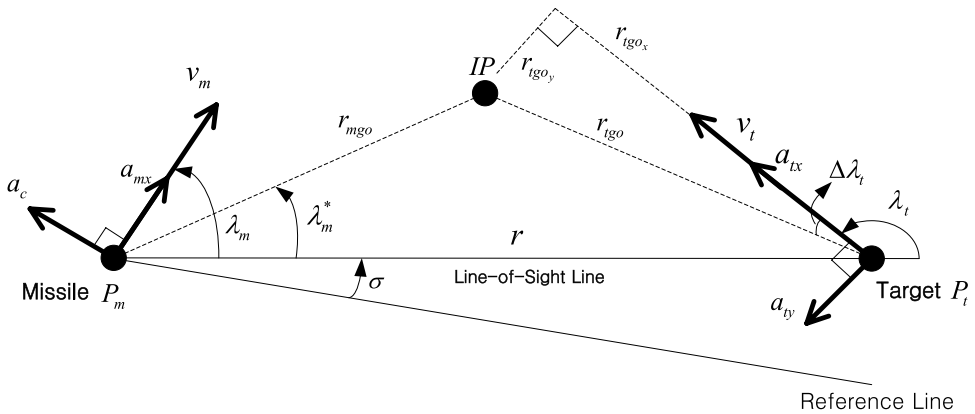


**Fig. 2** Engagement geometry considering interceptor and target acceleration

**Assumption 5** The change in the flight path angle of the target is small during the engagement.

It is worth noting that these assumptions have been widely accepted in the field of guidance law design. Since the guidance design is a problem of controlling the target–missile relative kinematics by assuming that the missile and the target have fast internal dynamics, Assumption 1 is reasonable to handle the guidance problem [1–4, 20]. In Assumption 2, the gravity-free assumption is commonly valid in the guidance design because the gravity is a known value, and it can be compensated in a guidance loop in an open-loop manner [1–4, 20]. Additionally, a ballistic target typically travels with an extremely high speed around 1–2 km/s during the terminal homing phase, and the detection range of the target by a seeker is very short due to its low radar cross-section (RCS) characteristic. It brings the fact that the homing time is extremely short under this engagement scenario. Therefore, when engaging a high-speed target such as a ballistic threat, the altitude change during the engagement is usually small. In that sense, it is reasonable to assume that the ballistic coefficient and the gravity almost remain constant during the engagement. Regarding Assumption 3, if a ballistic target is controlled by aerodynamic fins, acceleration response (i.e., the turn rate) becomes slow at a high altitude of over 10 km since the air density is very low. In that case, from the fact that the terminal homing time is extremely short and the turn rate of the target is slow during the engagement, it is reasonable to assume that the current target maneuver will be maintained until the interception. For Assumption 4, in practice, the actual longitudinal acceleration of the missile is nonlinearly varying according to the changes in the velocity and angle-of-attack. The thrust and aerodynamic drag mainly cause the variation of the longitudinal acceleration. However, during the gliding phase of the missile (after the propellant is burnt out), the velocity change is not significant, and it can be predicted by acceleration profiles [18]. Besides, if the missile is flying at a high altitude, this variation can be further reduced due to the absence of aerodynamic drag. Therefore, it is commonly acceptable to assume that the axial acceleration is maintained at an appropriate constant value during the engagement. Finally, Assumption 5 lies in the fact that the turn rate of the target is usually small due to its high speed, even though a large target acceleration is generated intended for trajectory shaping.

Figure 2 shows the relative engagement geometry between the interceptor missile and the target in the terminal homing phase. The notations $P_m$ and $P_t$ represent the positions of the missile and the target at an arbitrary time $t$, respectively. The parameters $v_m$ and $v_t$ denote the speeds of the missile and the target. Besides, $a_{tx}$ represents the longitudinal acceleration of the target, which acts parallel to $v_t$. The notation $a_{ty}$ denotes the lateral acceleration of the target, and this acceleration acts perpendicular to $v_t$. Similarly, $a_{mx}$ represents the longitudinal acceleration of the missile, which acts along the velocity vector of the missile. Additionally, $a_c$ represents the lateral acceleration of the missile, which can be considered as the control input of the missile system. The variable $\sigma$ denotes the LOS angle between the missile and the target. The relative range between the missile and the target is denoted by $r$. The variables $r_{mgo}$ and $r_{tgo}$ are defined as the predicted flight distances to be traveled by the missile and the target along with the collision triangle $P_m - IP - P_t$ until the interception.

The notation $\Delta\lambda_t$ is the predicted change in the look angle of the target caused by its lateral acceleration during the engagement. The variables $\lambda_m$ and $\lambda_t$ are the look angle of the missile and the target, respectively. From Fig. 2 with the definitions mentioned above, the closing velocity and the LOS rate at the current flight time are defined as follows:

$$\dot{r} = v_t \cos\lambda_t - v_m \cos\lambda_m, \tag{10}$$

$$r\dot{\sigma} = v_t \sin\lambda_t - v_m \sin\lambda_m. \tag{11}$$

### 3.2 Determination of Desired Look Angle

In the engagement scenario considered in this paper, the collision triangle for accomplishing the interception of the high-speed maneuvering target is created, as $P_m - IP - P_t$ in Fig. 2. Accordingly, if the missile approaches the target along the collision course $\lambda_m = \lambda_m^*$, then the missile can intercept the target without any corrective maneuver (i.e., $a_c = 0$). On the collision triangle $P_m - IP - P_t$, the following condition holds by the law of sine.

$$\frac{r_{tgo}}{\sin\lambda_m^*} = \frac{r_{mgo}}{\sin\left(\lambda_t + \Delta\lambda_t\right)} = \frac{r}{\sin\left(\lambda_t + \Delta\lambda_t - \lambda_m^*\right)}. \tag{12}$$

For convenience, let us define the reference frame where the current velocity direction of the target is defined as the $x$-axis (refer to Fig. 2). Under Assumption 5, the change in the flight path angle of the target is small during a short homing time. Therefore, in that case, the predicted flight distance to be traveled by the target in the $x$-axis of the reference frame is much longer than one in the $y$-axis of the reference frame, as $r_{tgo_x} \gg r_{tgo_y}$. This fact implies the condition of $\Delta\lambda_t \ll 1$.

Under the condition of $\Delta\lambda_t \ll 1$, the linearized kinematics of the target with respect to the reference frame can be determined as follows

$$\frac{d^2 r_{tgo_x}}{dt^2} = a_{tx} = -\frac{\rho S_{ref} C_D}{2m_t}\left(\frac{dr_{tgo_x}}{dt}\right)^2 = -\frac{\rho g}{2\beta}\left(\frac{dr_{tgo_x}}{dt}\right)^2, \tag{13}$$

$$\frac{d^2 r_{tgo_y}}{dt^2} = a_{ty}. \tag{14}$$

Note that in this derivation, the longitudinal acceleration caused by aerodynamic drag along the $x$-axis is only considered. In Eq. (13), the parameters $\rho$, $S_{ref}$, $C_D$, $m_t$, and $g$ denote the air density, the target reference area, the drag coefficient, the target mass, and the gravitational acceleration, respectively. Besides, the parameter $\beta$ in Eq. (13) represents the ballistic coefficient, which is defined as

$$\beta = \frac{m_t g}{S_{ref} C_D}. \tag{15}$$

Note that the linearized kinematics of the target, as given in Eq. (13), becomes an ODE with constant coefficients.

Hereafter, finding the solution of the above ODE will be explained. We first define a new variable as

$$dr_{tgo_x}/dt = v_{tx}. \tag{16}$$

Substituting the definition of the new variable into Eq. (13) yields the following equation.

$$\int \frac{1}{v_{tx}^2} dv_{tx} = \int -\frac{\rho g}{2\beta} dt. \tag{17}$$

By integrating Eq. (17) and setting the current target velocity as the initial value, the closed-form solution of the target velocity in the $x$-axis direction can be determined as

$$v_{tx}(\tau) = \frac{v_t}{1 + \frac{\rho g}{2\beta} v_t (\tau - t)}, \tag{18}$$

where the variable $\tau$ denotes an independent variable that lies in the range of values as $t \le \tau \le t_f$. Additionally, by further integrating Eq. (18), the closed-form solution of $r_{tgo_x}$ can be obtained as follows:

$$r_{tgo_x} = \int_t^{t_f} \frac{v_t}{1 + \frac{\rho g}{2\beta} v_t (\tau - t)} d\tau = \frac{2\beta}{\rho g} \ln\left(1 + \frac{\rho g}{2\beta} v_t t_{go}\right). \tag{19}$$

Similarly, we can determine the closed-form solution of $r_{tgo_y}$. Since the lateral acceleration of the target is assumed to be a constant value by Assumption 3, and the initial velocity in the $y$-axis direction is zero (i.e., $v_{ty} = 0$), the closed-form solution of $r_{tgo_y}$ can be obtained from the well-known solution of the rectilinear motion of the constant acceleration, as follows:

$$r_{tgo_y} = \frac{1}{2} a_{ty} t_{go}^2. \tag{20}$$

If the missile approaches the target along the collision course $\lambda_m = \lambda_m^*$, then the missile can intercept the target without any corrective maneuver (i.e., $a_c = 0$). Therefore, on the collision course, it can be assumed that the missile has the longitudinal acceleration only. The closed-form solution of $r_{mgo}$ can be obtained using the solution of the rectilinear motion of the constant acceleration, as below.

$$r_{mgo} = v_m t_{go} + \frac{1}{2} a_{mx} t_{go}^2. \tag{21}$$

Then, by substituting Eqs. (19), (20), and (21) into Eq. (12), we can determine the desired look angle allowing us to achieve the collision course, as follows:

$$\lambda_m^* = \sin^{-1}\left(\frac{r_{tgo}}{r_{mgo}} \sin\left(\lambda_t + \Delta\lambda_t\right)\right), \tag{22}$$

where

$$r_{tgo} = \sqrt{r_{tgo_x}^2 + r_{tgo_y}^2} = \sqrt{\left[\frac{2\beta}{\rho g} \ln\left(1 + \frac{\rho g}{2\beta} v_t t_{go}\right)\right]^2 + \frac{1}{4} a_{ty}^2 t_{go}^4}, \tag{23}$$

$$\Delta\lambda_t = \tan^{-1}\left(\frac{r_{tgo_y}}{r_{tgo_x}}\right) = \tan^{-1} \frac{a_{ty} \rho g t_{go}^2}{4\beta \ln\left(1 + \frac{\rho g}{2\beta} v_t t_{go}\right)}. \tag{24}$$

As can be seen in Eq. (22), the information on the missile and target state variables such as $v_m$, $a_{mx}$, $v_t$, $\beta$, $a_{ty}$, and $\lambda_t$ is required to determine the desired look angle of the missile for achieving the collision course. Additionally, the environmental parameters such as the air density $\rho$ and the gravitational acceleration $g$, and the time-to-go $t_{go}$ information are needed. Among the required parameters to calculate the desired look angle, the missile state variables can be measured by a built-in navigation system, and the target state variables can be adequately estimated from a dedicated guidance filter [25] using the information on seeker measurements. Then, the remaining term is the time-to-go, and it is usually calculated by utilizing the distance formula: the relative range over the closing velocity as

$$t_{go} = \frac{r}{v_c}, \tag{25}$$

where $v_c = -\dot{r}$. Here, it is worth noting that this calculation method has been developed based on the assumption that a missile and a target are moving with constant speeds. Therefore, if this method is applied for calculating the time-to-go under the engagement scenario considered in this study, a severe time-to-go estimation error is unavoidable. Such time-to-go estimation error could not only affect the accuracy of the calculation of the desired look angle but could also affect the performance of the proposed method eventually. Because of this reason, an accurate time-to-go calculation method that fits well the ballistic missile defense scenario is required in order to determine the desired look angle as precisely as

possible. In the following subsection, the proposed time-to-go calculation method will be discussed.

### 3.3 Proposed Time-to-Go Calculation Method

As can be seen from the collision triangle $P_m - IP - P_t$ in Fig. 2, there is a geometric relationship between the relative range and the predicted flight distances to be traveled by the missile and the target, as follows:

$$r_{mgo}\cos\lambda_m^* + r_{tgo_x}\cos\left(\pi-\lambda_t\right) + r_{tgo_y}\cos\left(\lambda_t-\frac{\pi}{2}\right) = r. \tag{26}$$

By substituting the expressions of $r_{mgo}$, $r_{tgo_x}$, and $r_{tgo_y}$, which are derived in the previous subsection, into Eq. (26), a nonlinear equation with respect to the time-to-go can be obtained. The time-to-go can then be determined by solving this nonlinear equation. However, this nonlinear equation is too complicated to obtain a time-to-go solution, and it is difficult to understand a solution space of the nonlinear equation. In other words, it is hard to check whether or not the solution of this nonlinear equation exists. Hence, instead of directly using Eq. (26), an approximate nonlinear equation based on a reasonable assumption is utilized to determine the time-to-go in this study.

In particular, for a surface-to-air missile intended to intercept a high-speed maneuvering target, terminal homing guidance generally follows an accurate guidance handover from appropriate mid-course guidance to form a collision course to the target as close as possible. That is to overcome the limited maneuvering capability and short homing time against a ballistic threat at a high altitude. Accordingly, the angle between $\lambda_m$ and $\lambda_m^*$ (defined as the heading error) is usually small at the beginning of the terminal homing phase. Besides, as the interceptor missile approaches the target, the current look angle gradually converges to the desired look angle required to shape the collision triangle (i.e., $\lambda_m \to \lambda_m^*$). These facts allow using the approximation of $\lambda_m \approx \lambda_m^*$. Based on this approximation, we have the following equation from Eq. (26).

$$r_{mgo}\cos\lambda_m - r_{tgo_x}\cos\lambda_t + r_{tgo_y}\sin\lambda_t = r. \tag{27}$$

By substituting Eqs. (19) through (21) into Eq. (27), the approximate nonlinear equation with respect to the time-to-go can be obtained as follows:

$$f\left(t_{\mathrm{go}}\right) = \frac{1}{2}\left(a_{ty}\sin\lambda_t + a_{mx}\cos\lambda_m\right)t_{\mathrm{go}}^2 + v_m\cos\lambda_m t_{\mathrm{go}} - \frac{2\beta\cos\lambda_t}{\rho g}\ln\left(1+\frac{\rho g v_t}{2\beta}t_{\mathrm{go}}\right) - r = 0. \tag{28}$$

By solving Eq. (28), the time-to-go can be determined. To this end, the existence of feasible solutions of the time-to-go (i.e., $t_{\mathrm{go}} \geq 0$) should be checked. And then, one of the feasible solutions would be the estimated remaining time of interception at the current time. To examine the existence of the feasible solutions, the approximate nonlinear equation as given in Eq. (28) is rearranged as

$$\underbrace{\left[\frac{1}{2}\left(a_{ty}\sin\lambda_t + a_{mx}\cos\lambda_m\right)t_{\mathrm{go}} + v_m\cos\lambda_m\right]t_{\mathrm{go}}}_{g(t_{\mathrm{go}})} = \underbrace{\frac{2\beta\cos\lambda_t}{\rho g}\ln\left(1+\frac{\rho g v_t}{2\beta}t_{\mathrm{go}}\right) + r}_{h(t_{\mathrm{go}})}. \tag{29}$$

From Eq. (29), when the terminal homing guidance phase is initiated with an accurate guidance handover from proper mid-course guidance, the initial engagement condition at the beginning of the terminal homing phase nearly lies on the collision course as shown in Fig. 2. Therefore, it can be generally assumed as $0.5\pi < \lambda_t < 1.5\pi$, $-0.5\pi < \lambda_m < 0.5\pi$ and $\dot{r} < 0$ (thus, $\cos\lambda_m > 0$, $\cos\lambda_t < 0$).

Under the engagement conditions as mentioned above, the general patterns of $g\left(t_{\mathrm{go}}\right)$ and $h\left(t_{\mathrm{go}}\right)$ can be shown in Fig. 3. We can readily observe that the pattern of $g\left(t_{\mathrm{go}}\right)$ can be altered according to the sign of $a_{ty}\sin\lambda_t + a_{mx}\cos\lambda_m$, and when the relative range $r$ goes zero, the time-to-go also converges to zero. Additionally, it can be found that the existence of feasible solutions can be determined by shifting $h\left(t_{\mathrm{go}}\right)$ along the $y$-axis depending on the magnitude of the relative range $r$ and examining intersection points with $g\left(t_{\mathrm{go}}\right)$ for fixed $\lambda_t$, $\lambda_m$, and $a_{tx}$. As shown in Fig. 3a, there exists one possible solution $t_{go}^*$ that satisfies the condition $t_{\mathrm{go}} \geq 0$ if $a_{ty}\sin\lambda_t + a_{mx}\cos\lambda_m \geq 0$. Conversely, in the case of $a_{ty}\sin\lambda_t + a_{mx}\cos\lambda_m < 0$, as shown in Fig. 3b, $h\left(t_{\mathrm{go}}\right)$ and $g\left(t_{\mathrm{go}}\right)$ might not intersect for $t_{go} \geq 0$, depending on the magnitudes of $\lambda_t$, $\lambda_m$, $a_{tx}$, and $r$. This is because the engagement situation is changed to the tail-chasing ($\dot{r} > 0$) over time, so the relative range cannot be achieved. In other words, there is a maximum relative distance value $r_{\max}$ or maximum time-to-go $t_{\mathrm{go}_{\max}}$ for the existence of the solutions, depending on the magnitude of $\lambda_t$, $\lambda_m$, $a_{tx}$, and $r$. The value of $t_{\mathrm{go}_{\max}}$ is the root of $f'(t_{\mathrm{go}}) = 0$, and the value of $r_{\max}$ is easily obtained by substituting $t_{\mathrm{go}_{\max}}$ into $h\left(t_{\mathrm{go}}\right)$. In the case of $r > r_{\max}$, the ballistic target cannot be intercepted by the intercept missile. However, since the value of $r$ is usually less than $r_{\max}$, there might exist two possible solutions, as shown in Fig. 3b. In that case, the minimum value of the two possible solutions should be selected as the solution (i.e., $t_{\mathrm{go}}^*$). This is because the time-to-go should converge to zero when the relative range $r$ goes to zero.

Since the function $f(t_{\mathrm{go}})$ is given by a nonlinear equation, it is challenging to obtain a solution analytically. Thus, we utilize a numerical approach, such as the Newton–Raphson

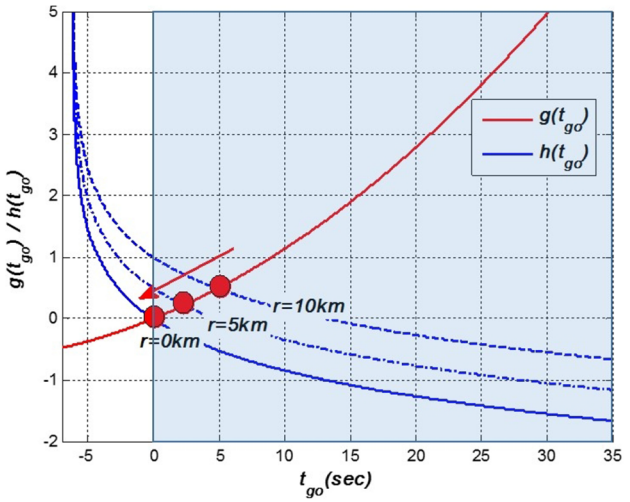


**(a)** Condition I: $a_{ty}\sin\lambda_t + a_{mx}\cos\lambda_m \geq 0$

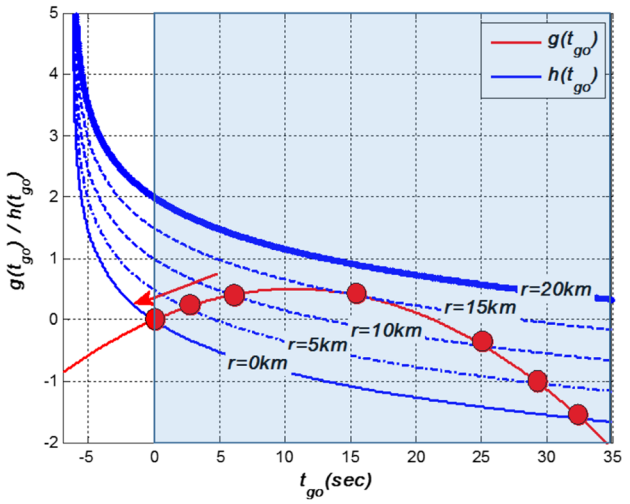


**(b)** Condition II: $a_{ty}\sin\lambda_t + a_{mx}\cos\lambda_m < 0$

**Fig. 3** The solutions of the time-to-go equation

method, to find the solutions in this paper. This method finds the solutions using Eq. (30). Therefore, the function $f(t_{\text{go}})$ should be differentiable. If the value of $f(t_{\text{go}})$ becomes zero or a very small value near solutions, this method fails to find solutions because they are diverging. Additionally, if there are multiple solutions, there is a possibility to find a wrong solution depending on initial values.

$$x_{n+1} = x_n - \frac{f(x)}{f'(x)}. \tag{30}$$

If $a_{ty}\sin\lambda_t + a_{mx}\cos\lambda_m \geq 0$, it can be seen that the function $f(t_{\text{go}})$ is differentiable, and there is no point where $f'(t_{\text{go}}) = 0$ because the function $f(t_{\text{go}})$ is monotonically increasing for $t_{\text{go}} \geq 0$. Since there exists one solution, we can find one exact solution $t^*_{\text{go}}$. In the case of $a_{ty}\sin\lambda_t + a_{mx}\cos\lambda_m < 0$, we can limit the time range as $\left[0, t_{\text{go}_{\max}}\right]$ to find the solution, then the function $f(t_{\text{go}})$ is monotonically increasing in this interval. It implies that there is no point where $f'(t_{\text{go}}) = 0$. In that case, there exist two possible solutions, but the one exact solution $t^*_{go}$ can be determined in the time interval $\left[0, t_{\text{go}_{\max}}\right]$. By setting the initial value $x_0$ of the solution as $r/v_c$, the number of iterations could be reduced while finding solutions using the Newton–Raphson method.

### 3.4 Proposed Guidance Command

Once the estimated time-to-go and the desired look angle are calculated, the proposed guidance command can then be determined. Hereafter, we will introduce the proposed guidance command that utilizes the information on the desired look angle and the time-to-go, as determined in the previous subsections. At first, by applying the estimated time-to-go $t^*_{\text{go}}$ and the state variables of the interceptor missile and the target into Eq. (22), the desired look angle $\lambda^*_m$ achieving the collision course can be determined. As mentioned in Sect. 2, the desired LOS rate corresponding to $\lambda^*_m$ can be determined using the LOS rate definition, as given in Eq. (11). The resultant desired LOS rate is given as

$$\dot{\sigma}^* = \frac{v_t\sin\lambda_t - v_m\sin\lambda^*_m}{r} = \frac{1}{r}\left[v_t\sin\lambda_t - v_m\left(\frac{r_{tgo}}{r_{mgo}}\sin\left(\lambda_t + \Delta\lambda_t\right)\right)\right]. \tag{31}$$

By substituting the expression of $\dot{\sigma}^*$, as given by Eq. (31), into the BPNG command form, as given in Eq. (1), we have the final form of the proposed guidance command as

$$\begin{aligned} a_c &= N' v_c(\dot{\sigma} - \dot{\sigma}^*) \\ &= N' v_c\left\{\dot{\sigma} - \frac{1}{r}\left[v_t\sin\lambda_t - v_m\left(\frac{r_{tgo}}{r_{mgo}}\sin\left(\lambda_t + \Delta\lambda_t\right)\right)\right]\right\}. \end{aligned} \tag{32}$$

As can be seen in Eq. (32), the proposed guidance law could be understood as a kind BPNG law. Compared to other BPNG laws, the proposed guidance law has a unique form of the bias term. The role of this term is to compensate for the collision course deviation due to the target and interceptor missile motions. Therefore, under the proposed guidance law, the missile can approach the target along the accurate collision course as close as possible, even in the presence of the target and interceptor missile motions. This favorable characteristic of the proposed method could minimize the control energy compared to PNG. This fact will be verified through numerical simulations in the next section.

## 4 Simulation Results

In this section, numerical simulations are performed to investigate the characteristics and the performance of the proposed guidance law as well as to verify the performance improvement of the proposed method over the existing methods such as PNG and APNG.

### 4.1 Performance Verification of the Proposed Guidance Law

In this simulation study, we consider an extreme engagement scenario where the ballistic target maneuvers in the lateral direction for trajectory shaping, and the ballistic target undergoes a large deceleration due to aerodynamic drag. The simulation parameters are provided in Table 1. Additionally, the effective navigation ratio is set to $N' = 3$ as the default value.

Figure 4a shows the engagement trajectory under the proposed guidance law. In the simulation, the terminal homing guidance begins at the relative range of about 7 km, and the homing time takes about 3 s. The interception is made at an altitude of about 8 km, as shown in Fig. 4a.

Figure 4b presents the longitudinal and lateral accelerations imposed on the ballistic target in the numerical simulation. The lateral acceleration is recorded as 10 g, which causes the change in the flight path angle of the target, as shown in Fig. 4a. We can observe that the longitudinal deceleration is nonlinearly varying in the range of values from $-30$ to $-15$ g, due to aerodynamic drag. Because of this deceleration, the closing velocity is also significantly varying from 2500 to 1800 m/s, as shown in Fig. 4c. This observation confirms the premises of our study, as discussed in Sect. 3: the speeds of the target and the missile will be considerably varying, in the engagement scenario where a surface-to-air missile intended to intercept a ballistic target.

Figure 4b depicts the variation of the look angle of the missile during the engagement. As shown in Fig. 4d, the heading error (i.e., $\lambda_m - \lambda_m^*$) at the beginning of the terminal homing phase is recorded as 15 °. From the result obtained, it can also be observed that the heading error gradually decreases as time goes, and the heading error converges to zero at around 2.5 s. It implies that the missile lies on the collision course after 2.5 s. Next, Fig. 4e shows the converging patterns of the heading error $\lambda_m - \lambda_m^*$ for various effective navigation ratio. As sown in Fig. 4e, it can be observed that the convergence rate increases as $N'$ increases.

Figure 4f provides the difference between the LOS rate and the desired LOS rate. To achieve the collision course, the LOS rate error should be nullified. As shown in Fig. 4f, it can be observed that the LOS rate eventually converges to the desired LOS rate within 2.5 s. It indicates that the proposed guidance law is appropriately working to accomplish the interception condition. Figure 4g compares the guidance commands under the proposed method and the classical PNG. From the result, we can readily observe that the proposed guidance command converges to zero as the missile approaches the target. This is because the proposed guidance law can drive the missile to follow the accurate collision course. Therefore, once the missile lies on the collision course, no maneuvering is required in the proposed method. This characteristic could be a benefit in terms of ensuring an operational margin of maneuverability to cope with uncertainties during the engagement. On the other hand, 35 g maneuvering is observed in the PNG case, as shown in Fig. 4g. Since PNG assumes constant speeds of the target and the missile, PNG guides the missile to follow an inaccurate collision course. That is why a huge maneuver is required in PNG. This property is adverse in terms of enlarging the capturability of the ballistic target since the guidance command under PNG can be easily saturated by the command limitation.

Figure 4h presents a comparison of the time-to-go calculation methods. As shown in Fig. 4h, the conventional method undergoes a severe estimation error. On the other hand, the proposed method can accurately calculate the time-to-go as close as the actual value, as shown in Fig. 4h. It implies that we can compute the predicted intercept point precisely by utilizing the proposed time-to-go calculation method.

**Table 1** Test scenario

| Parameter | Value |
|---|---|
| $P_{t0}$ | (10 km, 10 km) |
| $v_{t0}$ | 2000 m/s |
| $\gamma_{t0}$ | 200 deg |
| $\beta$ | 2392 kgf/m$^2$ |
| $a_{ty}$ | 10 g |
| $P_{m0}$ | (5 km, 5 km) |
| $v_{m0}$ | 1000 m/s |
| $a_{mx}$ | −2 g |

### 4.2 Performance Comparison with PNG and APNG

Figure 5a and b presents the command variations under PNG and the proposed guidance, according to changes in the effective navigation ratio. This is to show the advantage of acceleration profiles for the proposed method over PNG. At the initial, the maximum required acceleration under the proposed guidance is huge, except for the case $N' = 3$. However, regardless of the effective navigation ratio, the total control energy usage ($\Delta v = \int_0^{t_f} |a_c| \, dt$) is significantly reduced under the proposed method. Additionally, it can be observed that as the intercept missile flies at a high altitude,

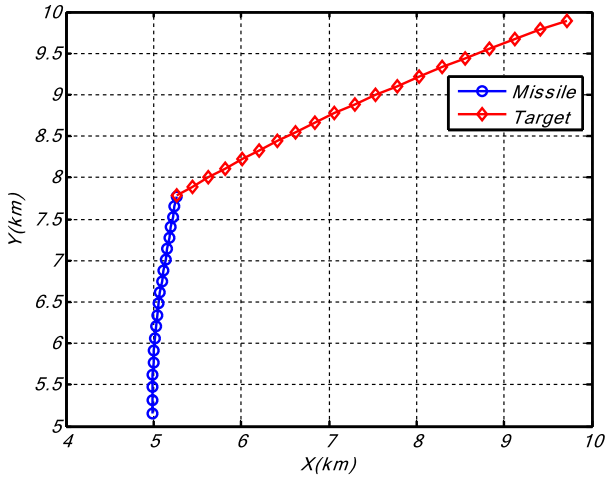


**(a)** Engagement trajectory

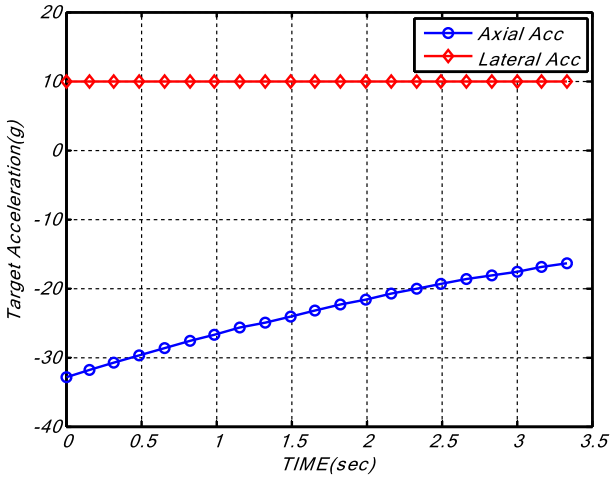


**(b)** Target acceleration

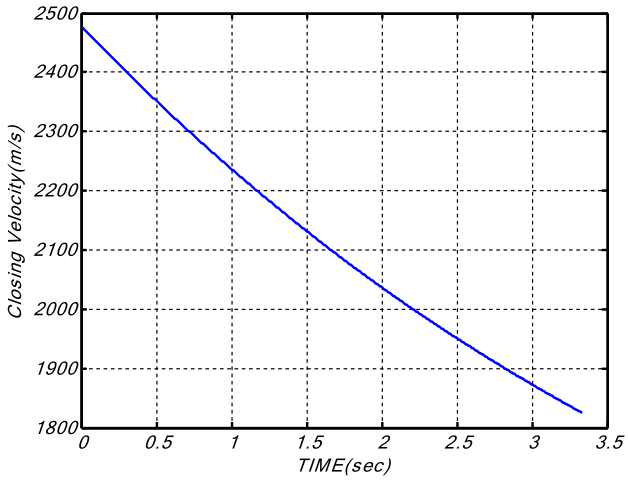


**(c)** Closing velocity

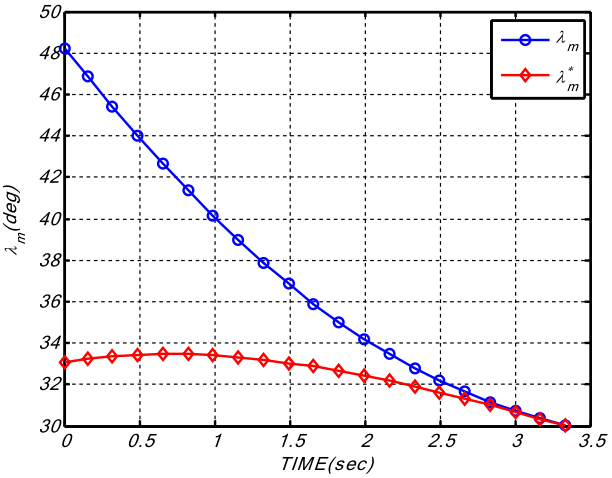


**(d)** $\lambda_m$ variation

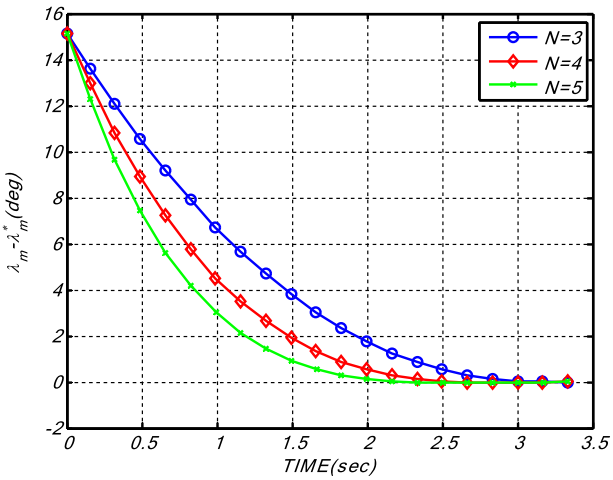


**(e)** $\lambda_m - \lambda_m^*$ variation according to $N$ value

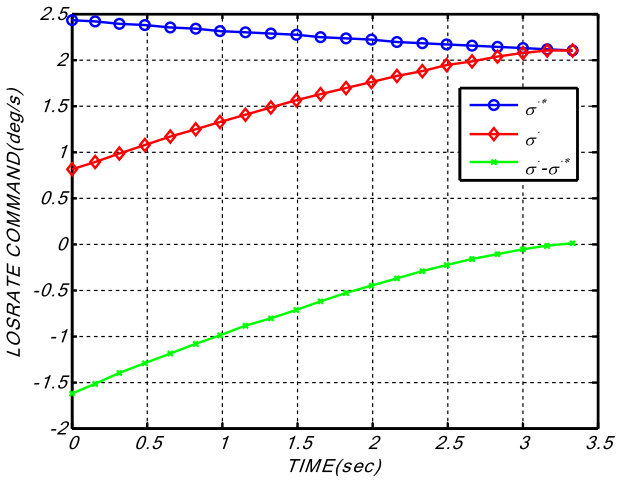


**(f)** LOS rate command variation ( $\dot{\sigma} - \dot{\sigma}^*$ )

**Fig. 4** Simulation results of the engagement scenario

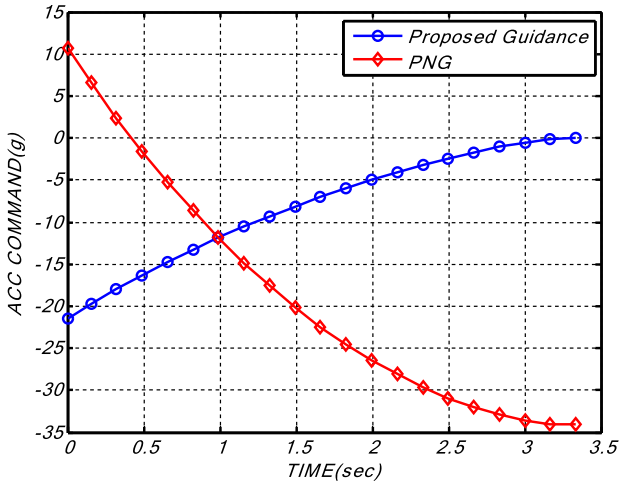


**(g)** Guidance command comparison

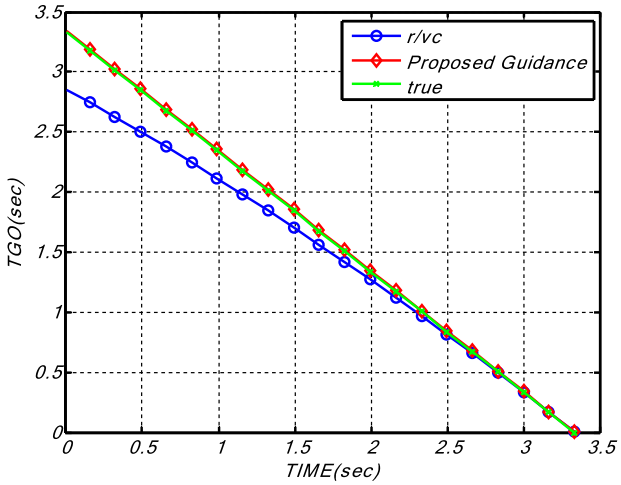


**(h)** $t_{go}$ calculation results.

**Fig. 4** (continued)

the acceleration demand decreases and converges to almost zero. This characteristic of the proposed guidance will be beneficial to overcome the limited maneuvering capability and short homing time, especially when engagement occurs at a high altitude such as ballistic target interception case.

Figure 5c and d shows the capture regions for PNG and the proposed guidance, according to the changes in the heading error and the target lateral acceleration, with the maneuverability limit of the interceptor missile. The input range of the heading error and the target lateral acceleration are chosen as $[-30 \ -30 \ \text{deg}]$ and $[0 \ -20 \ g]$, respectively. If the miss distance is smaller than 1 m, we assume that the target is intercepted by the missile in the capturability analysis. As shown in Fig. 5c and d, we can readily observe that the capture region of the proposed guidance is considerably broader than that of PNG. In this analysis, the capturability is evaluated by the kinematic interception. Therefore, if we further consider the unknown disturbances, such as the wind and target maneuvers, this gap will be larger.

Figure 6 shows a comparison of the guidance commands under the proposed method and APNG for the different initial $\lambda_m - \lambda_m^*$ cases. In the case of $\lambda_m - \lambda_m^* = 0$ deg, we can readily observe that the proposed guidance command becomes nearly zero at the moment of intercept. Unlike the proposed guidance, APNG requires about 4 g at the beginning of the homing guidance, and the guidance command does not converge to zero at the terminal time. In the simulation, the terminal acceleration under APNG is recorded as 3 g, as shown in Fig. 6a. This is because a certain acceleration command is always required to compensate for a nonlinear deceleration and lateral acceleration of the ballistic missile in the case of APNG. Moreover, the gimbal angle of the intercept missile is about 30 deg in this simulation so that the effect of not compensating for the component perpendicular to the LOS of the missile longitudinal deceleration (which is about 1 $g$) is also included.

Similarly, in the case of $\lambda_m - \lambda_m^* = 15$ deg, the proposed guidance command converges to zero as the relative range decreases to zero. On the other hand, APNG does not allow this property. As shown in Fig. 6b, APNG demands more acceleration at the terminal time than the proposed method. The simulation results confirm that the proposed guidance outperforms than APNG in the engagement situations considered in this paper. APNG is an optimal guidance law derived from the linearized engagement kinematics under the assumption that the target lateral acceleration is constant. In the augmented term (i.e., $0.5N'a_T$), $a_T$ represents the components of the longitudinal deceleration and the lateral acceleration perpendicular to the LOS vector. It means that this method relies on the information of the target accelerations only. However, since the proposed guidance considers all the acceleration components of the ballistic missile and the interceptor missile when generating the guidance command and it can accurately estimate the time-to-go using a newly proposed method, the exact collision triangle can be achieved by the proposed method. In this way, the acceleration demand could be reduced in the proposed method compared to APNG.

## 5 Conclusion

In the ballistic missile defense scenario, a tactical ballistic missile flies in a quasi-ballistic trajectory with a high speed, and it usually undergoes a considerable deceleration due to aerodynamic drag. Additionally, it may perform an evasive

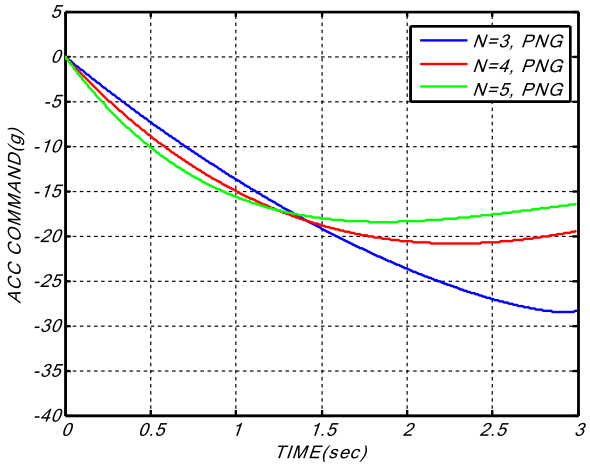


**(a)** PNG command variation according to $N$

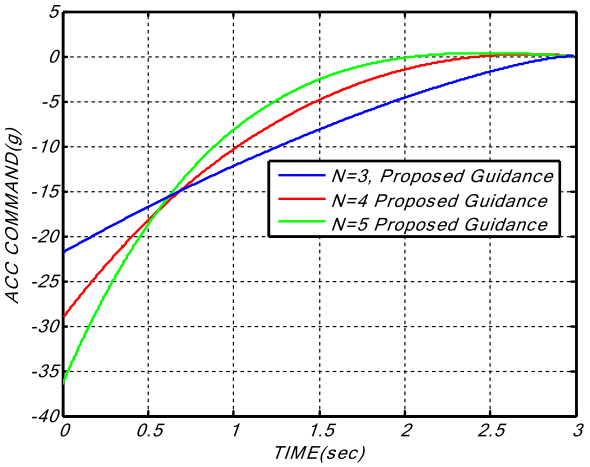


**(b)** Proposed Guidance command variation according to $N$

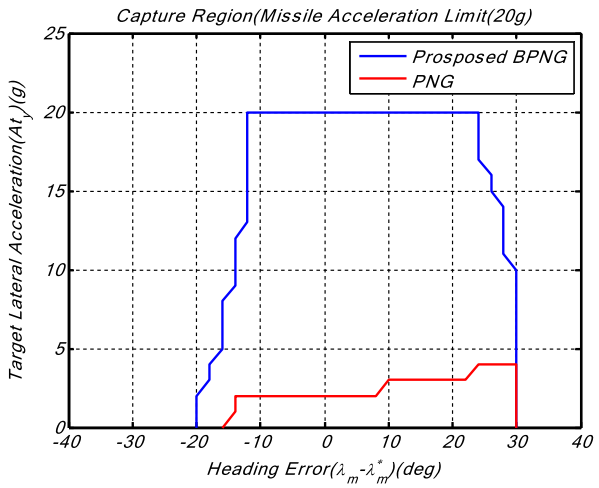


**(c)** Capture Region(20g Limit)

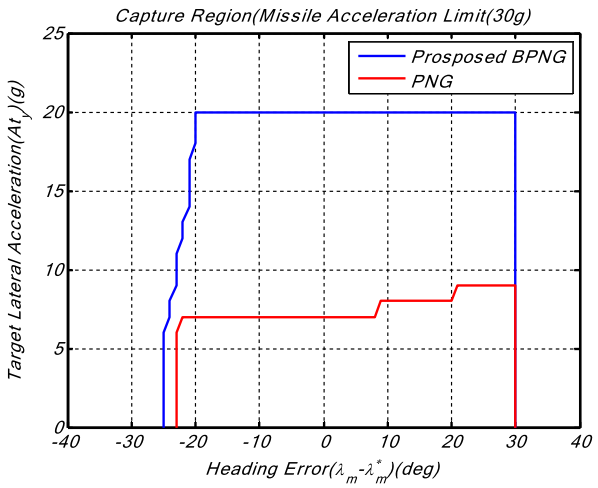


**(d)** Capture Region(30g Limit)

**Fig. 5** Performance comparison with PNG

maneuver to avoid an attack of an interceptor missile. In this extreme engagement scenario, the classical proportional navigation guidance (PNG) results in performance degradation: a large guidance command generated in the vicinity of the target leads to the command saturation, thereby resulting in severe miss distance.

In this paper, new homing guidance was developed to resolve the issue. Through the closed-form trajectory solutions of the bias PNG (BPNG) command, we first deduced the relationship between the desired LOS rate in the BPNG command and the desired look angle corresponding to the collision triangle. Next, we developed the methods that estimate the accurate time-to-go and the desired look angle leading to the accurate collision course for a ballistic target. By utilizing the desired look angle and the desired LOS rate definition, we finally derived a state-feedback form of a guidance law that can make the interceptor missile follow the predicted collision course without any corrective maneuvers near the end of the flight.

The simulation results showed that the look angle of the missile converged to the desired value under the proposed method, as intended. Accordingly, it was confirmed that the accurate collision course was accomplished by the proposed method. Additionally, from the results obtained, it was also observed that the estimated time-to-go by the proposed method was almost identical to the actual value. Besides, it was confirmed that the proposed method was able to considerably reduce unnecessary maneuvering in the terminal homing phase, compared to PNG. The performance improvement of the proposed method over the APNG was also verified through numerical simulations. For implementing the proposed method, the information on target state variables is required. However, it could be precisely estimated using a dedicated guidance filter with sensor measurements

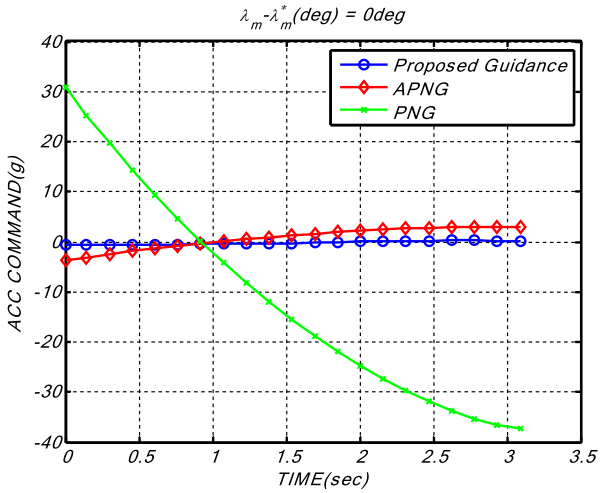


**(a)** Command comparison( $\lambda_m - \lambda_m^* = 0\,\text{deg}$ )

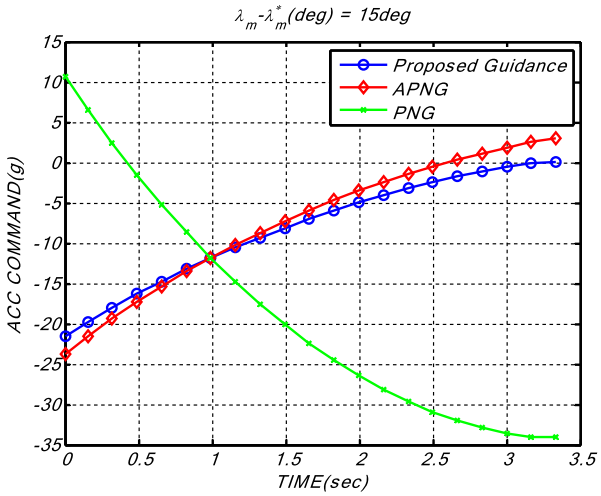


**(b)** Command comparison( $\lambda_m - \lambda_m^* = 15\,\text{deg}$ )

**Fig. 6** Performance comparison with APNG

provided by a high-range resolution onboard seeker and a ground radar.

## References


1. Murtaugh SA, Criel HE (1966) Fundamentals of proportional navigation. IEEE Spectr 3(12):75–85
2. Bryson A, Ho YC (1975) Applied optimal control. Wiley, New York
3. Zarchan P (2012) Tactical and strategic missile guidance, 6th edn. American Institute of Aeronautics and Astronautics, Washington
4. Lin CF (1991) Modern navigation, guidance, and control processing. Prentice Hall, New Jersey
5. Kreindler E (1973) Optimality of proportional navigation. AIAA J 11(6):878–880
6. Jeon IS, Lee JI (2010) Optimality of proportional navigation based on nonlinear formulation. IEEE Trans Aerosp Electron Syst 46(4):2051–2055
7. "SS-26 Iskander." Missile threat, https://missilethreat.csis.org/missile/ss-26-2/.
8. Chadwick WR (1985) Miss distance of proportional navigation missile with varying velocity. J Guid Control Dyn 8(5):662–666
9. Arbenz K (1970) Proportional navigation on nonstationary targets. IEEE Trans Aerosp Electron Syst 4:455–457
10. Ryu MY, Lee CH, Tahk MJ (2015) Command shaping optimal guidance laws against high-speed incoming targets. J Guid Control Dyn 38(10):2025–2033
11. Gazit R, Gutman S (1991) Development of guidance laws for a variable-speed missile. Dyn Control 1(2):177–198
12. Gazit R (1993) Guidance to collision of a variable-speed missile. The first IEEE regional conference on aerospace control systems. Westlake Village, CA, USA
13. Baba Y, Yamaguchi M, Howe RM (1993) Generalized guidance law for collision courses. J Guid Control Dyn 16(3):511–516
14. Gutman S (2005) Applied min-max approach to missile guidance and control. American Institute of Aeronautics and Astronautics, Washington
15. Baba Y, Takehira T, Takano H (1994) New guidance law for a missile with varying velocity, AIAA Guidance, Navigation, and Control Conference. Scottsdale, AZ, USA, AIAA-94-3565-CP
16. Reisner D, Shima T (2013) Optimal guidance to collision law for an accelerating exoatmospheric interceptor missile. J Guid Control Dyn 36(6):1695–1708
17. Shima T, Golan OM (2012) Exo-atmospheric guidance of an accelerating interceptor missile. J Franklin Inst 349(2):622–637
18. Cho HJ, Ryoo CK, Tahk MJ (1999) Implementation of optimal guidance laws using predicted missile predicted missile velocity profiles. J Guid Control Dyn 22(4):579–588
19. Lee CH, Kim TH, Tahk MJ (2013) Interception angle control guidance using proportional navigation with error feedback. J Guid Control Dyn 36(5):1556–1561
20. Jung YS, Lee JI, Lee CH, Tahk MJ (2019) A new collision control guidance law based on speed control for kill vehicle. Int J Aeronaut Space Sci Guid 20:792–805
21. Shukla US, Mahapatra PR (1989) Optimization of biased proportional navigation. IEEE Trans Aerospace Elect Syst AES-25(1):73–80
22. Imado F, Kuroda T, Tahk MJ (1998) A new missile guidance algorithm against a maneuvering target, AIAA guidance, navigation, and control conference and Exhibit. Boston, MA, USA, AIAA-09-4114
23. Shima T, Golan OM (2007) Head pursuit guidance. J Guid Control Dyn 30(5):1437–1444
24. Ghosh S, Ghose D, Raha S (2014) Retro-PN based simultaneous salvo attack against higher speed nonmaneuvering targets. IFAC Proc Vol 47(1):34–40
25. Ghosh S, Mukhopadhyay S, Routray A (2012) New state and measurement models for endo-atmospheric tracking of ballistic target using seeker measurement. IEEE Trans Aerosp Electron Syst 48(2):1192–1209